**Proceedings of the ASME 2018 International Mechanical Engineering Congress and Exposition**
**IMECE2018**
**November 9-15, 2018, Pittsburgh, PA, USA**

# IMECE2018-87313

# EFFECT OF OSCILLATING WATER COLUMN CHAMBER INCLINATION ON THE PERFORMANCE OF A SAVONIUS ROTOR

**Deepak D. Prasad**
The University of the South Pacific
Suva, Fiji

**Mohammed Rafiuddin Ahmed**
The University of the South Pacific
Suva, Fiji

**Young-Ho Lee**
Korea Maritime & Ocean University
Busan, South Korea

## ABSTRACT

The global power potential of the waves that hit all the coasts worldwide has been estimated to be in the order of 1 TW. On an average, each wave crest transmits 10-50 kW/m of energy and this corresponds to 15 to 20 times more energy per meter than wind or solar energies. Wave energy is environmentally friendly and is the most consistent of all the intermittent sources. While wind, solar and wave are all intermittent, wave is the most consistent. Availability of waves is 90% compared to 30% for wind and solar energy. The oscillating water column (OWC) is the most investigated wave energy converter (WEC). OWC is a partially submerged hollow structure positioned, either vertically or at an angle. The bi-directional flow of air above the water column is used to drive a turbine. Majority of the OWC devices have chambers which are perpendicular to the incident waves. These conventional OWCs suffer severely from flow separation that occurs at the sharp corners of the chamber. In order to address this issue, researchers have proposed inclining the chamber at an angle with respect to the incident waves. This improves the flow characteristics. In addition to this, the flow in the chamber which ultimately decides the turbine performance, also increases. In the present study, the effect of OWC inclination on rotor performance was numerically studied using commercial computational fluid dynamics (CFD) code ANSYS CFX. The results highlight that the 55° inclined OWC showed improved performance when compared to the conventional OWC and current OWC. The maximum power for the inclined OWC was 13% higher than that recorded for the rotor in the current OWC and 28% than that recorded in the conventional OWC at mean wave condition. The 55° inclined OWC recorded peak rotor power of 23.2 kW which corresponded to an efficiency of 27.6% at the mean sea state. The peak power and efficiency at maximum sea state was 26.5 kW and 21.5% respectively. Higher oscillation was observed in the 55° inclined OWC. The combination of increased flow rate and energy in the flow lead to better performance of the 55° inclined OWC.

## INTRODUCTION

The present demands for the use of clean energy sources for electricity production as a counter measure against the global phenomenon of climate change are motivating researchers to pursue renewables. The change in the weather pattern brought about by global warming threatens the livelihood of everyone. A report by Inter-governmental Panel on Climate Change [1] highlighted increase of 0.85°C in the global averaged combined land and ocean surface temperature from 1880 to 2012. The increase in global temperature has led to a rise in sea level due to the melting of polar ice caps. The rising sea level threatens small low-lying islands.

One of the green and clean energy sources is waves. It is estimated that the worldwide power potential of waves hitting the coastline is 1 TW [2]. This represents energy per wave crest of 10-50 kW [3]. The energy of the waves can be extracted using a suitable WEC. OWC which is a matured technology has been used widely for wave energy extraction. Majority of OWC devices have chambers that are perpendicular to the incident waves. These conventional OWCs suffer severely from flow separation that occurs at the sharp corners of the chamber which leads to energy losses. The function of the chamber is to capture the energy of the incident waves as effectively as possible. This first stage energy conversion is crucial in determining the performance of the OWC. In order to address

this issue, researchers have proposed inclining the chamber at an angle with respect to the incident waves.

Ram et al. [4] experimentally studied the flow characteristics in an inclined bend-free OWC device. The dynamic pressure measurements and water level fluctuations inside the capture chamber were recorded for different inclination angles. The results showed an increase in the velocity of air flowing in the capture chamber as the inclination angle is reduced. They also recorded higher water level fluctuations in the chamber at lower angles. The authors stated that the best inclination angles were between 45° and 55°. Patel et al. [5] studied 65° inclined OWC device employing a Savonius rotor. The inclined OWC reduces the influence of reflected waves on the performance of the rotor. The tests were conducted at varying water depths and wave frequencies and the authors reported peak performance for all the cases at a frequency of 0.8 Hz. The study highlighted strong dependence of performance on wave period. Iino et al. [6] investigated the effect of inclination on water oscillation characteristics in the OWC. The authors developed a mechanical one degree-of-freedom oscillator model of the inclined OWC. The model was validated with experimental results obtained from wave tank testing of a cylindrical OWC at 90°, 45° and 18.4° inclinations. The paper highlighted that the resonance period was prolonged by the reduced restoring force as the direction of motion changed and concluded that changing the direction of motion affected the oscillation characteristics of OWCs.

The literature clearly highlights that there is a lack of information regarding the effect of inclination on OWC performance. There is no consensus on which angle of inclination leads to optimum performance. Furthermore, the optimum inclination angle is device dependent. It can not be accepted without verification that the optimum inclination angle of one OWC device will necessarily be the same for another. Each device is unique with its' unique optimum inclination angle. As a result of this, the present work is intended to investigate the effect of inclination on the OWC performance employing a Savonius rotor numerically using ANSYS-CFX. A numerical wave tank (NWT) based on Navier-Stokes equations is employed to study the performance of a conventional OWC, an OWC optimized by Prasad et al. [7] (named current OWC) and inclined OWCs. The waves in the NWT were generated using a piston type wave-maker. The wave climate generated is same as that reported by Ram et al. [8]. The mean wave height (*H)* and the mean wave period (*T)* used in the simulation were 2.00 m and 12.68 s respectively. The current numerical code used was previously validated against real sea data by the authors and can be found in Prasad et al. [9]. Secondly the performance of the 55° inclined OWC is further investigated at the minimum sea state ($H$ = 1.37 m and $T$ = 10.00 s) and maximum sea state ($H$ = 2.34 m and $T$ = 14.39 s). The rotor power, rotor efficiency and flow characteristics are presented and discussed in this paper.

## METHODOLOGY

Initially a 1:14 scale model of the conventional OWC was constructed and tested at varying wave conditions. For the experiment the Savonius rotor had a blade entry angle of 30°. Two rotor diameters of 70 mm and 90 mm were tested. The results of this study can be found in ref. 7. The next step was to conduct numerical studies on the same OWC and optimize the OWC geometry and the rotor geometry. The CFD code was validated against experimental results. The OWC geometry upon optimization yielded the current OWC configuration as shown in Fig. 3. For the rotor optimization, the blade entry angles tested were 20°, 30° and 40°. The rotor diameter was also varied from 80 mm to 10 mm at increments of 5 mm. The best rotor configuration was found out to be rotor with blade entry angle of 40° and diameter of 100 mm. The dimensions of the full scale Savonius rotor is shown in Fig. 2. Once the optimization was complete the performance of the full scale OWC is investigated as part of this study.

The solid modelling of all the parts was done using NX 8 UniGrapics software. The schematic of the NWT is shown in Fig. 1. The entire length of the computational domain was 700 m. The OWC was positioned at 1.5λ (where λ is the wavelength) from the wave-maker and 3λ from the back-wall. Lakshmynarayanan et al. [10] in their work had the inlet and the back wall at 1.5λ and 2λ respectively from the model. The total length of the wave-maker region and the wave damping zone is 100 m. The width of the NWT was 28 m while the water depth ($h$) was 18 m. The inlet of the OWC facing the incident waves was located 2.1 m below the mean water level. At this depth, the Savonius rotor was fully submerged. The dimensions of the Savonius rotor are shown in Fig. 2. The dimensions in Figs. 2 and 3 are in meters. The length of the rotor is 2.8 m and the blade entry angle is 40°.

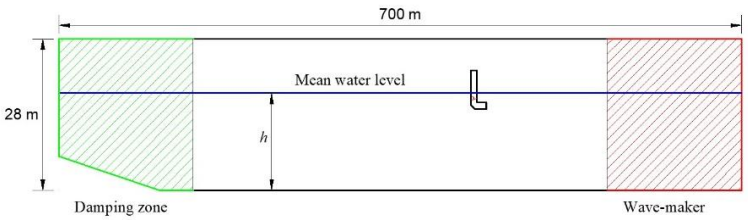


Fig. 1 Schematic diagram of the NWT.

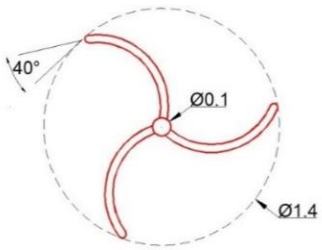


Fig. 2 Schematic diagram of the Savonius rotor.

The schematic diagrams of the three OWCs are shown in Fig. 3. The current OWC configuration was obtained by optimizing the OWC from experiments conducted by Prasad et al. [7]. The inclination angle, $\theta$, is varied in the present work from 45° to 65° at increments of 5° to find the optimum angle.

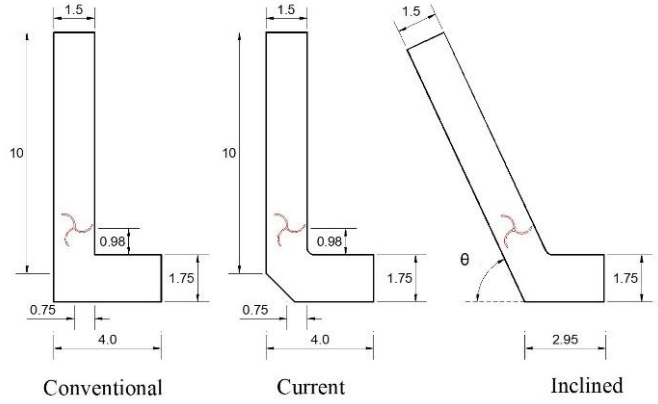


Fig. 3 Schematic of the three OWC configurations.

ICEM CFD software was used for the discretization of the model using hexahedral meshing. This grid generation scheme allows for user-defined meshing which is of high mesh quality. The meshing for the NWT, OWC and the Savonius rotor are shown in Fig. 4. The mesh was refined near the mean water level region to capture the air-water interface accurately. The total number of nodes was approximately 800,000.

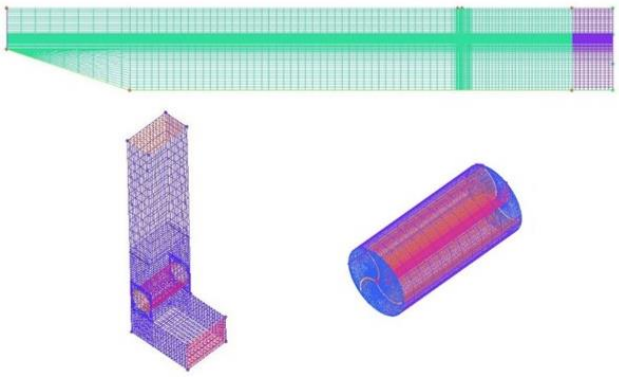

Fig. 4 Mesh scheme for the NWT, OWC and Savonius rotor.

For carrying out the numerical work, commercial computational fluid dynamics (CFD) code ANSYS CFX was employed. It solves the Reynolds Averaged Navier Stokes Equation (RANSE).The governing equations solved are mass and momentum conservation and given by equations 1 and 2 (Lal and Elangovan [11]).

$$\frac{\partial \rho}{\partial t} + \nabla \bullet \rho v = 0 \tag{1}$$

$$\frac{\partial}{\partial t} \rho v + \nabla \bullet \rho v = -\nabla p + \nabla \bullet \tau = 0 \tag{2}$$

The air-water free surface was captured using VOF method. The two critical boundary conditions that needed to be captured were the dynamic boundary condition and the kinematic free surface boundary condition as given in equations 3 and 4 respectively (Maguire [12] and Falnes [13]).

$$g\eta + \left[\frac{\partial \phi}{\partial t}\right]_{z=\eta} = 0 \tag{3}$$

$$\left[\frac{\partial^2 \phi}{\partial t^2} + g\frac{\partial \phi}{\partial z}\right]_{z=0} = 0 \tag{4}$$

The volume of fluid (VOF) method which is an interface capturing method, was used to capture the free surface. In VOF method, each cell is considered to be full of fluid of varying fractions. This adds another governing equation, proposed and used by Finnegan and Goggins [14]:

$$\frac{\partial q_i}{\partial t} + u_1 \frac{\partial q_i}{\partial x} + u_2 \frac{\partial q_i}{\partial y} = 0 \tag{5}$$

In the equation 5, $i$ is the two fluids present ($i$ = 1 and 2), $q_i$ is the volume fraction of fluid $i$ with $\sum_{i=1}^{2} q_i = 1$. Assuming $q_1$ is the volume fraction of water then there can be three possible conditions:

$$q_i = q_1 = \begin{cases} 1 & cell\ full\ of\ water \\ 0 < q_1 < 1 & air - water\ interface \\ 0 & cell\ has\ no\ water \end{cases} \tag{6}$$

For further details of the numerical method, the authors' previous work (Prasad et al. [9]) can be referred. The computational domain was divided into three domains: the NWT, the OWC and the rotor, as shown in Fig. 5. The wave-maker region was the moving mesh region. The inlet of the NWT which is named as plate was assigned a specific displacement using user-defined expression given in equation 7. An opening boundary type was assigned to the top of the NWT. The volume fraction for both water and air was specified along with relative pressure of 0 Pa. No-slip boundary condition was assigned to the bottom wall and the back wall of this domain. For the OWC domain, the top side of the chamber was assigned the boundary condition of opening and the side from which the waves entered the domain was set as an interface. The remaining sides of the domain were specified with no-slip condition. The rotor domain was treated as a rotating domain and the speed of the Savonius rotor was specified. The inner walls of the OWC were modeled as walls with free-slip condition. The rotor blades were also assigned no–slip condition. A 1:3 slope was incorporated to dampen the reflected waves from the back wall as proposed by Elangovan [15].

$$xdis = A\sin(\omega t) \quad (7)$$

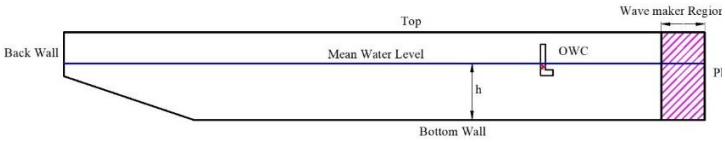


Fig. 5 Schematic of the computational domain.

Parallel computer network was used to carry out the numerical work. The computer was equipped with Intel(R)_Xeon(R)_CPU X5650 processor. There were 12 cores in total and the RAM size was 16 GB. Since the formation of the waves is time dependent and unsteady, therefore a transient simulation was performed using $k$-$\varepsilon$ turbulence model. The time discertization of the equations was achieved with the implicit second order Backward Euler scheme. For advection scheme and turbulence numerics, high resolution options were chosen. The time step between each iteration was chosen as 0.05 s and the coefficient loop was selected as 7.

## RESULTS AND DISCUSSION

Initially the influence of grid size on the results was investigated. Grid independence test was conducted using 400,000, 800,000 and 1,200,000 nodes. The power recorded at rotational speed of 30 rpm at the mean wave condition ($H$ = 2.00 m and $T$ = 12.68 s) for different grid sizes is presented in table 1. The grid size of 800,000 was chosen for all the simulations. Increasing the number of nodes to 1,200,000 only showed a deviation of 1% in the recorded power. The additional number of nodes did not provided any benefit in accuracy apart from increasing the simulation time. The wave elevation in the NWT was compared with linear wave theory (LWT) as shown in Fig. 6. It can be seen that the current numerical code is able to predict the wave profile accurately. The exact wave conditions used in the present work were successfully validated by the authors [16]. After the validation, they conducted studies on the performance of Savonius rotors in that work.

Table 1 Effect of grid size on the rotor power for current OWC

| Grid Size | Rotor Power (kW) |
|---|---|
| 400,000 | 9.35 |
| 800,000 | 9.64 |
| 1,200,000 | 9.73 |

The performance of the rotor at varying rotational speeds for the mean sea state for current OWC is shown in Fig. 7. The power increases as the speed of the rotor increases. It reaches a peak at 60 rpm and then drops significantly from this point onwards. The peak is an indication of optimum operating condition. At this speed the interaction between the rotor and the incident waves is maximum which results in maximum power production. The maximum power and the resulting efficiency recorded at best operating point are 18.85 kW and 22.44% respectively.

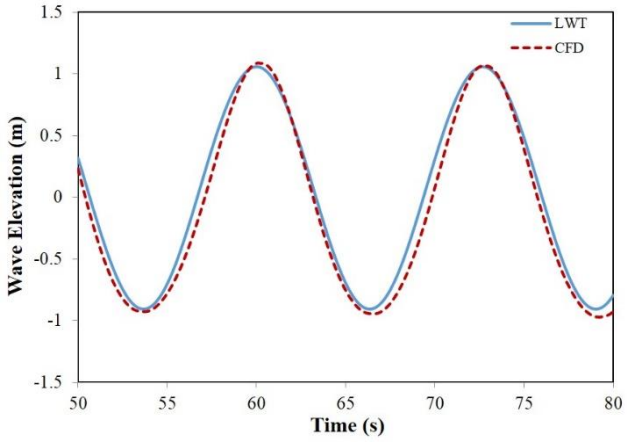


Fig. 6 Comparison of wave elevation obtained using CFD and LWT at the mean sea state.

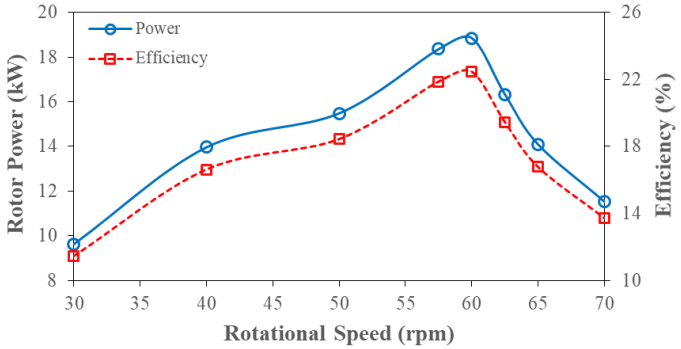


Fig. 7 Performance of the current OWC at the mean wave condition.

The performance characteristics of the inclined OWCs at the mean wave condition are shown in Fig. 8. The simulations were only performed at four rotor speeds. This speed range was selected based on the peak occurring at 60 rpm, as shown in Fig. 7. The OWC performance increase from 45° to 55° and starts to decrease.

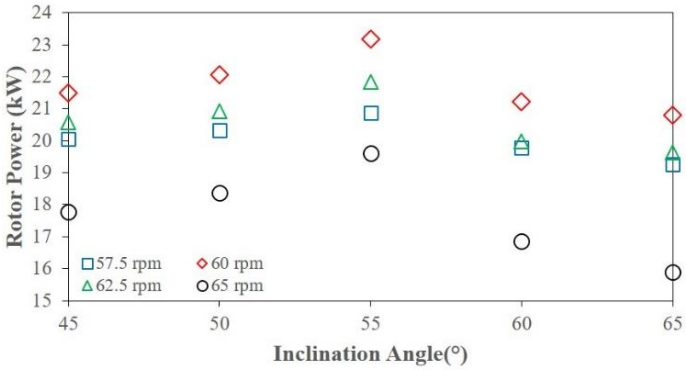


Fig. 8 Effect of OWC inclination angle on the rotor power at mean wave condition at different rotor rpms.

The 55° inclined OWC recorded the highest power at all the speeds. The maximum power and efficiency recorded for the 55° inclined OWC were 23.2 kW and 27.6% respectively. Furthermore, the performance of the 55° inclined OWC was compared with the conventional OWC and the current OWC as shown in Fig. 9. The average increase in power for the 55° inclined OWC with respect to the conventional OWC and the current OWC were 45% and 27% respectively.

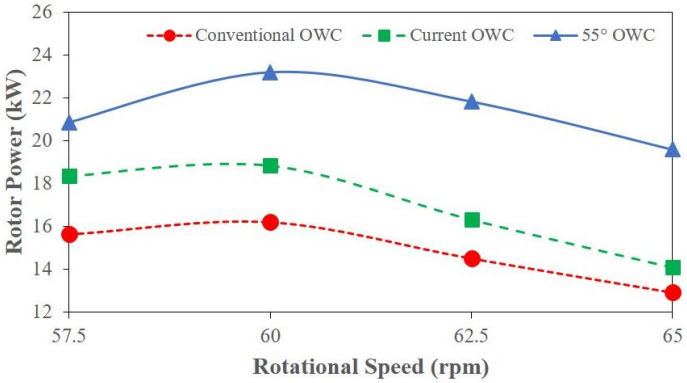


Fig. 9 Performance comparison of the 55° inclined OWC with the conventional and the current OWC at mean wave condition.

The flow characteristics in the OWC chamber for the current OWC and the 55° inclined OWC at the same instant are shown in Fig. 10. It is observed that the energy of the flow received by the rotor was slightly higher in the 55° inclined OWC. In addition to this, there was no re-circulating flow observed in region *A* for the 55° inclined OWC.

The increase in the power for the 55° inclined OWC is due to higher run-up into the OWC chamber and hence higher volume of water. The direction of motion of the water surface in the chamber changes by inclining the OWC. By inclining the OWC, the gravity force has lesser effect and affects the oscillation characteristics of the water column [6]. This simply means that the flow rate is higher when compared to the other two configurations.

The water oscillations in the chamber for the 55° inclined OWC and the conventional OWC are shown in Fig. 11. A comparison of the oscillations for the two cases makes it clear that the 55° inclined OWC experiences higher oscillations compared to the conventional OWC, resulting in a higher volume flux in the capture chamber. This results in an increase in the dynamic pressure as well as the flow rate of water. The combination of increased flow rate and energy of the flow lead to better performance of the 55° inclined OWC. For the 55° inclined OWC, the reflections from the wall also reduce significantly which improve the flow characteristics inside the capture chamber and hence the performance of the 55° inclined OWC.

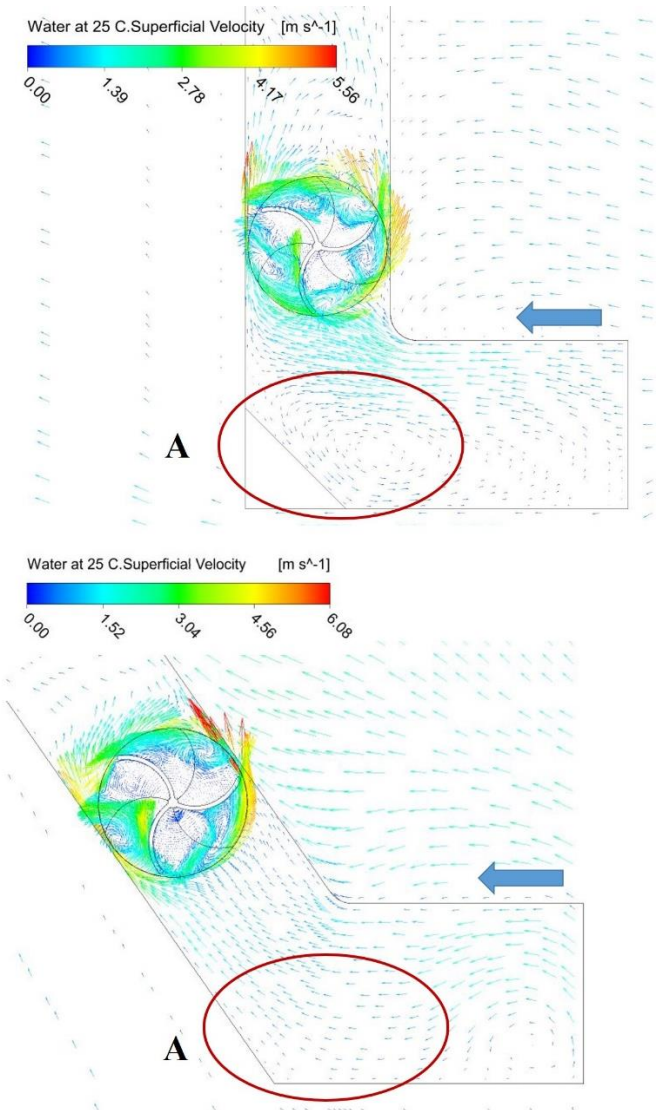


Fig. 10 Flow characteristics in the current OWC and the 55° inclined OWC.

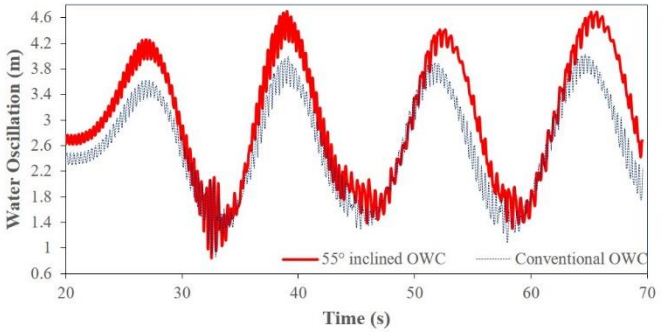


Fig. 11 Water oscillations in the conventional OWC and the 55° inclined OWC at the mean sea state.

Furthermore, the performance of the 55° inclined OWC was also investigated at the minimum sea state ($H$ = 1.37 m and $T$ = 10.00 s) and the maximum sea state ($H$ = 2.34 m and $T$ = 14.39 s) and the results for the rotor power are depicted in Fig. 12. The peak power at the minimum and the maximum sea states occurs at 57.5 rpm and 55 rpm respectively. As expected, the highest power was produced at the maximum sea state. The peak power and efficiency at maximum sea state were found to be 26.5 kW and 21.5% respectively. The results obtained in the present study indicate that the best inclination angle is 55°. It is important to understand that this optimum inclination angle is unique to this device only.

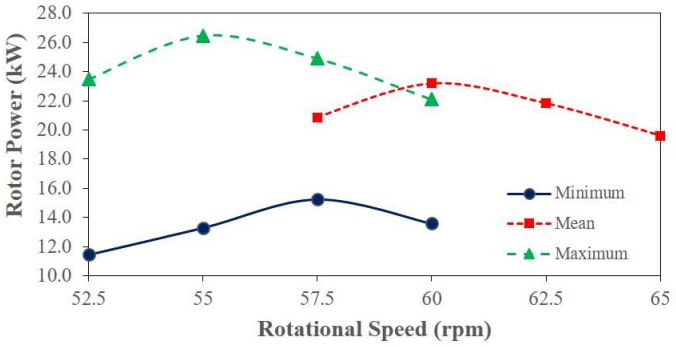


Fig. 12 Performance of 55° inclined OWC at different sea states.

Finally the efficiencies achieved in the present work is compared with similar past works and the comparison is presented in table 2. For the present work, the rotor diameter was 1.4 m and the rotor width was 2.8 m. This is comparable to the rotor dimensions of Zullah et al. [18]. They employed a rotor which was 2.0 m in diameter and 3.0 m wide. The efficiency obtained in the present work is comparable.

Table 2 Efficiency comparison between present work and similar past works.

| Reference | Maximum Efficiency (%) | Comments |
|---|---|---|
| Zullah et al [17] | 12.64 | OWC employing 30° helical blade Savonius rotor as a direct drive turbine |
| Zullah et al [18] | 18.58 | OWC employing Savonius rotor as a direct drive turbine |
| Bikas et al [19] | 6 to 8 | Ocean surface mounted Savonius rotor |
| **Present work** | **27.6** | 55° OWC employing Savonius rotor with blade entry angle of 40° as a direct drive turbine at mean wave condition |
| **Present work** | **21.5** | 55° OWC employing Savonius rotor with blade entry angle of 40° as a direct drive turbine at maximum wave condition |

## CONCLUSIONS

The effect of inclining the OWC on the rotor performance was investigated and the 55° inclined OWC showed improved performance when compared to the conventional OWC and the current OWC. The maximum power for the 55° inclined OWC was 27% higher than that recorded for the rotor in the current OWC and 45% than that recorded in the conventional OWC at mean wave condition. The 55° inclined OWC recorded peak rotor power of 23.2 kW which corresponded to an efficiency of 27.6% at mean sea state. The peak power and efficiency at maximum sea state was 26.5 kW and 21.5% respectively. Higher oscillations were observed in the 55° inclined OWC. The combination of increased flow rate and energy of the flow lead to the better performance of the 55° inclined OWC.

## REFERENCES

[1] Stocker, T. F., Qin, D., Plattner, G. K., Tignor, M., Allen, S. K., Boschung, J., Nauels, A., Xia, Y., Bex, V. and Midgley, P. (eds). 2013, Climate Change 2013: The Physical Science Basis. In: IPCC 2013 - Contribution of Working Group I to the Fifth Assessment Report of the Intergovernmental Panel on Climate Change. 1535 pp. Cambridge University Press, Cambridge, United Kingdom and New York, NY, USA, 1535 pp.

[2] Panicker, N., 1976, Power Resource Potential of Ocean Surface Waves. In: *Proceedings of the Wave and Salinity Gradient Workshop*. pp. J1-J48.

[3] Sundar, V., 2015, O*cean Wave Mechanics – Applications in Marine Structures*. John Wiley & Sons Limited.

[4] Ram, K., Ahmed, M. R., Zullah, M. and Lee, Y. H., 2016, Experimental Studies on the Flow Characteristics in an Inclined Bend Free OWC Device. *Journal of Ocean Engineering and Science*, pp. 77-83.

[5] Patel, S., Ram, K., Ahmed, M. R. and Lee, Y. H., 2011, Performance Studies on an Oscillating Water Column Employing a Savonius Rotor. *Science China Technological Sciences*, 54(7), pp. 1674-1679.

[6] Iino, M., Miyazaki, T., Segawa, H. and Iida, M., 2016, Effect of Inclination on Oscillation Characteristics of an Oscillating Water Column Wave Energy Converter. *Ocean Engineering*, 116, pp. 226-235.

[7] Prasad, D., Kim, C. G., Kang, H. G., Ahmed, M. R. and Lee, Y. H., 2017, Performance and Flow Characteristics of Single and a Novel Double Oscillating Water Column Devices. *Journal of Mechanical Science and Technology,* 31(12): pp. 5879-5886.

[8] Ram, K., Narayan, S., Ahmed, M. R., Nakavulevu, P. and Lee, Y. H., 2014, In Situ Near-shore Wave Resource

 

Assessment in the Fiji Islands. *Energy for Sustainable Development*, 23, pp. 170-178.

[9] Prasad, D., Ahmed, M. R., Lee, Y. H. and Sharma, R. N., 2017, Validation of a Piston Type Wave-maker using Numerical Wave Tank. *Ocean Engineering*, 131, pp. 57-67.

[10] Lakshmynarayanana, P., Temarel, P. and Chen, Z., 2016, Hydroelastic Analysis of a Flexible Barge in Regular Waves Using Coupled CFD-FEM Modelling. In: *Proceedings of the 5th International Conference on Marine Structures (MARSTRUCT)*. Southampton, UK.

[11] Lal, A. and Elangovan, M., 2008, CFD Simulation and Validation of Flap Type Wave-maker. *World Academy of Science, Engineering and Technology,* 46, pp.76–82.

[12] Maguire, A. E. *Hydrodynamics, Control and Numerical Modelling of Absorbing Wavemakers*., 2011, PhD Dissertation. The University of Edinburgh, UK.

[13] Falnes, J. Ocean Waves and Oscillating Systems. 2002. Cambridge Univ. Press.

[14] Finnegan, W. and Goggins, J., 2012, Numerical Simulation of Linear Water Waves and Wave-Structure Interaction. *Ocean Engineering*, 43, pp. 23-31.

[15] Elangovan, M., 2011, Simulation of Irregular Waves by CFD. *World Academy of Science, Engineering and Technology - International Journal of Mechanical, Aerospace, Industrial, Mechatronic and Manufacturing Engineering*, 5(7), pp. 1379-1383.

[16] Prasad, D., Ahmed, M. R., Lee, Y. H. and Sharma, R. N., 2017, Studies on the Performance of Savonius Rotors in a Numerical Wave Tank. *Ocean Engineering*, 158, pp. 29-37.

[17] Zullah, M., Prasad, D., Choi, Y. and Lee, Y., 2009, Study on the Performance of Helical Savonius Rotor for Wave Energy Conversion. In: *Proceedings of the 10th Asian International Conference on Fluid Machinery*. Kuala Lumpur.

[18] Zullah, M. and Lee, Y., 2013, Performance Evaluation of a Direct Drive Wave Energy Converter Using CFD. *Renewable Energy*, 49, pp. 237-241.

[19] Bikas, G., Ramesh, H. and Vijaykumar, H., 2014, Study on Performance of Savonius Rotor Type Wave Energy Converter used in Conjunction Conventional Rubble Mound Breaker. *Ocean Engineering*, 89, pp. 62-68.